CHROM. 5051

FLOW OF He, Ar, AND CO_2 THROUGH A 200 ft. $\frac{1}{8}$ in. O.D. PORAPAK S (50–80 MESH) COLUMN AT 273° K

J. J. CZUBRYT* AND H. D. GESSER
Department of Chemistry, University of Manitoba, Winnipeg (Canada)
(Received August 11th, 1970)

SUMMARY

The flow of He, Ar, and CO_2 through a 200 ft. 1/8 in. O.D. Porapak S (50–80 mesh) column has been studied at 273° K. It was found that the gas flow cannot be completely described in terms of the existing relationships. Certain mechanisms must be postulated in order to explain some of the anomalies found in this study.

INTRODUCTION

In the previous article dealing with the effect of carrier gas nonideality and adsorption on the net retention volume of a solute[1], it was found that in the experiments using helium as a carrier gas, the experimental data at the highest pressures employed was inconsistent with the proposed mechanism of carrier gas adsorption. Without evidence this discrepancy was attributed to a secondary flow mechanism in which only helium can participate. It is the intent of this article to provide experimental evidence to support this view as well as to explore the question of carrier gas flow through this type of column (described in ref. 1) in terms of the existing theories and/or empirical relationships.

Due to compressibility, the carrier gas will experience acceleration as it travels down the column and consequently its velocity will increase with the distance. Texts treating fluid motion often describe the velocity profile by the Navier-Stokes equation[2,3]. Solution of this equation leads to the correct description of gas flow but as GIDDINGS[4] points out the intractable nature of this equation is beyond exact treatment for such complex flow space geometries as those found in a gas chromatographic column.

The flow of gas through a porous media is more practically described by an empirical relationship proposed by Darcy[5]. In terms of the apparent gas velocity u_a (using CARMAN's notation[5]) Darcy's Law states that for a flow of gas in the x direction

$$u_a = -\left(\frac{B_o}{\eta}\right)\frac{dP}{dx} \qquad (1)$$

where B_o is the specific permeability coefficient and η is the gas viscosity, and u_a is defined as[5],

$$u_a = Q/At \qquad (2)$$

* Holder of the National Research Council of Canada Studentship 1967–1968.

where Q, A and t are the volume of gas, the cross-sectional area of the porous media and the time, respectively. It has been pointed out on several occasions[4,6,7] that u_a is not the true velocity of the gas since the actual cross-sectional area of a porous media such as the gas chromatographic column through which gas can flow is $A\varepsilon$ where ε is the porosity of the media. Applying this correction to eqn. 1 and remembering that

$$F = uA\varepsilon \tag{3}$$

eqn. 1 can be expressed in terms of the flow rate (F) as follows

$$F = -\left(\frac{B_o A}{\eta}\right)\frac{dP}{dx} \tag{4}$$

For a gas chromatographic column where the carrier gas may be considered as ideal it can be shown that

$$F = \frac{F_o P_o}{P} \tag{5}$$

where F and F_o are the flow rates at points where the pressure is P and P_o respectively, the latter of which is the outlet pressure. Substitution of eqn. 5 into eqn. 4 and upon rearrangment we get

$$F_o P_o dx = -\left(\frac{B_o A}{\eta}\right) P dP \tag{6}$$

Integration between the limits of $x = 0$ and $x = L$ where the column pressures are P_i and P_o respectively followed by rearrangement gives

$$F_o = \left(\frac{B_o A}{2\eta L P_o}\right)(P_i^2 - P_o^2) \tag{7}$$

If the carrier gas is nonideal and can be approximated by the following equation of state

$$n = \frac{PV}{RT + B_{11}P} \tag{8}$$

then eqn. 6 will become

$$\frac{F_o P_o dx}{RT + B_{11}P_o} = -\left(\frac{B_o A}{\eta}\right)\left(\frac{P dP}{RT + B_{11}P}\right) \tag{9}$$

Integration between the same limits as above leads to

$$\frac{F_o}{1 + bP_o} = \left(\frac{B_o A}{\eta b^2}\right)[b(P_i - P_o) + \ln(1 + bP_o) - \ln(1 + bP_i)] \tag{10}$$

where b is merely the ratio B_{11}/RT. The ln terms are of the form $\ln(1 + x)$ and can be approximated by

$$\ln(1 + x) = \frac{2x}{2 + x} \tag{11}$$

This form of approximation is very good in that even for x having a value of 0.5 which is much higher than normally encountered, the difference between the actual value of

$\ln(1 + x)$ and the approximation is only -1.35 %. After making this approximation in eqn. 10 and algebraic rearrangement, the final expression becomes:

$$F_o = \left(\frac{B_o A}{\eta L P_o}\right)\left[(1 + bP_o)\left(\frac{P_i^2}{2 + bP_i} - \frac{P_o^2}{2 + bP_o}\right)\right] \tag{12}$$

In the limit when the carrier gas is ideal (*i.e.* $b = 0$), eqn. 12 reduces to eqn. 7.

The specific permeability (B_0) has the units of cm^2 but can also be expressed in Darcy units where 1 Darcy $= 9.87 \times 10^{-9}$ cm^2. It is related to the porosity (ε) which in turn is related to the nature of the packing material and column construction. The relating equation is the Kozeny-Carman eqn.[5] which has the form

$$B_o = \frac{d_p^2 \cdot \varepsilon^3}{36k(1 - \varepsilon)^2} \tag{13}$$

where d_p is the diameter of a sphere with the same specific surface as the particle so that for a spherical nonporous particles, d_p will be that of the particle diameter. k is a constant but is appears that for normal granular packed columns there are two distinct values of k that are in use.

In some publications the accepted value of k is 5.0 (refs. 4–6, 8, 9). Using this value eqn. 13 becomes

$$B_o = \frac{d_p^2 \cdot \varepsilon^3}{180(1 - \varepsilon)^2} \tag{14}$$

In other publications[7,10–14] the accepted value of k is very close to 4.17 thus making eqn. 13 become

$$B_o = \frac{d_p^2 \cdot \varepsilon^3}{150(1 - \varepsilon)^2} \tag{15}$$

Now, eqn. 15 has been referred to as the Blake-Kozeny equation[6,10,11] whereas eqn. 14 has been referred to as the Kozeny-Carman equation[4–6,9]. On occasions eqn. 15 has been called the Kozeny-Carman equation[13] as well as the Ergun equation[9]. It is not clear which of the two equations is the correct one since it appears that there exists sufficient experimental data to support them both[5,10,13].

For a GC column porosity can be defined as the fraction of the total volume which is accessible to the mobile phase, that is

$$\text{porosity} = \frac{V_M}{V_T} = \frac{V_M}{\pi r^2 L} \tag{16}$$

For porous materials V_M will contain it in the inter and the intraparticle volumes and consequently the porosity as defined by eqn. 16 is the total porosity or ε_T. The free space which is chiefly responsible for gas transport is the interparticle void. It follows then that the porosity contained in eqn. 14 or 15 is the interparticle posority (ε).

The two porosities can be related as follows:

$$\varepsilon_T = \varepsilon + \Delta \tag{17}$$

where Δ is the porosity arising from the porous nature of the material. For nonporous materials such as glass beads Δ vanishes and the two porosities become identical. The

interparticle porosity can range from 0.35 to 0.9, but for a fairly well packed column the value is very close to 0.4 (ref. 4). The value of 0.9 is encountered in unusual situations such as the aerogel columns[15].

Darcy's Law is applicable only to relatively low gas velocities, that is, in the region of laminar flow. As the gas velocity is increased the laminar flow becomes unstable and gives way to a flow of an erratic pattern which is generally known as turbulent flow. With the onset of turbulence there is an apparent decrease in permeability with increasing flow rate, that is higher pressure differences are required than that expressed by eqn. 7 or eqn. 12. The deviations are too large to be accounted for by the carrier gas nonideality (eqn. 12) or by the increase in viscosity, and can be explained by the loss of the gas kinetic energy through heat dissipation in the numerous eddies and cross-currents of turbulent flow. To account for this a quadratic velocity term is added to Darcy's relationship[4,5], that is

$$\frac{-\mathrm{d}P}{\mathrm{d}x} = au + bu^2 \tag{18}$$

The degree of turbulence can be estimated by a velocity dependant dimensionless term known as the Reynolds number (R_e), which has the form[4,7]

$$R_e = \frac{\rho u d_p}{\eta} \tag{19}$$

where ρ is the specific gravity of the gas. It should be pointed out that the product ρu will be constant throughout the entire column. According to GIDDINGS[4], turbulence develops gradually from a minor to a dominant role as R_e increases from 1 to 100. He further states that the departure from Darcy's Law when $R_e > 1$ constitutes evidence that turbulence is occurring, and at $R_e \simeq 1$ turbulence can be expected in only a few of the largest channels. GUIOCHON[7] on the other hand contends that the flow must be laminar at $R_e \sim 1$ and that Darcy's Law extends to $R_e = 10$ to 15. BIRD *et al.*[10] mention that for $\varepsilon < 0.5$ the Blake-Kozeny equation (which by their notation contains the integrated form of Darcy's Law) is valid up to $R_e/(1-\varepsilon) < 10$, or, if $\varepsilon \simeq 0.4$ then $R_e < 6$.

GUIOCHON points out that use can be made of Ergun's equation for calculating the permeability coefficient in the turbulent region. Using the present notation this relationship can be expressed as follows

$$\frac{1}{k} = \frac{150(1-\varepsilon)^2}{d_p^2\varepsilon^2} + \frac{1.75\rho u_o(1-\varepsilon)}{d_p\eta\varepsilon} \tag{20}$$

where k is a velocity dependent permeability coefficient and u_o is the column outlet velocity. By dividing both sides of eqn. 20 by ε and remembering that the resulting first term on the right hand side is actually $1/B_o$, eqn. 20 can be rewritten to give

$$\frac{1}{k\varepsilon} = \frac{1}{B} = \frac{1}{B_o} + \frac{1.75\rho u_o(1-\varepsilon)}{d_p\eta\varepsilon^2} \tag{21}$$

At relatively low pressures, the density can be approximated by

$$\rho = \frac{P_o M}{RT \times 10^3} \tag{22}$$

Substituting this relationship and the one expressed by eqn. 3 into eqn. 21, eqn. 21 reduces to

$$\frac{1}{B} = \frac{1}{B_o} + Y\left(\frac{M}{\eta}\right) F_o \tag{23}$$

where

$$Y = \frac{1.75 P_o(1-\varepsilon)}{RTA d_p \varepsilon^3 \times 10^3} \tag{24}$$

At constant P_o, Y is a constant which is independent of the nature of the carrier gas. F_o in eqn. 23 is expressed in cc/sec.

EXPERIMENTAL

The experimental apparatus and procedure has been described elsewhere[1]. All experiments were carried out at 273° K.

RESULTS AND DISCUSSION

The experiments from which the data is extracted will be designated by the carrier gas used. For example Ar I, Ar II and Ar III refer to three distinct experiments using argon as the carrier gas.

For simplicity of notation eqn. 12 can be rewritten to read

$$F_o = \chi\phi \tag{25}$$

where

$$\chi = \frac{BA}{\eta} \tag{26}$$

and

$$\phi = \frac{1}{P_o}(1 + bP_o)\left(\frac{P_i^2}{2 + bP_i} - \frac{P_o^2}{2 + bP_o}\right) \tag{27}$$

The method for calculating the B_{11} terms used in eqn. 12 or 27 was already described in ref. 1.

According to eqn. 25 and eqn. 26 the relationship between F_o and ϕ will be linear in the laminar flow region where B is constant. With the onset of turbulence where there is an apparent decrease in B, there will be a progressive decrease in the slope as ϕ increases and as the result a nonlinear departure from Darcy's Law will be observed. To test this relationship F_o (cc/min) was plotted against ϕ (atm) for three different carrier gases, namely, He, Ar, and CO_2. Figs. 1, 2 and 3 refer to He I, Ar (II and III) and CO_2 I, respectively. The helium plot shows a linear relationship throughout the entire experimental range. If for the present it can be assumed that $\varepsilon = 0.4$, then it appears that Darcy's Law is valid for the gas velocity range from 0 to about 120 cm/sec. This is quite consistent with the results obtained by HARGROVE AND SAWYER[16] for helium gas flowing through a glass bead column. They observed a linear relationship between F_o and ϕ (ideal gas) up to F_o of approx. 550 cc/min or in terms of gas velocity up to about 290 cm/sec.

In the case of Ar and CO_2 a straight line could be drawn through only four or five points. If it can be assumed that Darcy's Law is valid for this region, extrapolation of this line to cover the entire experimental range serves to indicate the deviation from this law. Since the line is extrapolated from the laminar flow region, its slope can serve to evaluate χ_o and in turn B_o. This is done below.

$\chi_o(\text{He}) = 0.55$ cc/min atm
$\chi_o(\text{Ar}) = 0.51$ cc/min atm
$\chi_o(CO_2) = 0.68$ cc/min atm

In order to convert these values to B_o, the following constants were used:

1 atm $= 1.0133 \times 10^6$ dynes/cm^2
$L = 6096$ cm
$A = 2.14 \times 10^{-2}$ cm^2
$\eta(\text{He}, 273) = 1.887 \times 10^{-4}$ g/cm·sec (ref. 17)
$\eta(\text{Ar}, 273) = 2.104 \times 10^{-4}$ g/cm·sec (ref. 17)
$\eta(CO_2, 273) = 1.380 \times 10^{-4}$ g/cm·sec (ref. 17)

The corresponding B_o values were calculated to be:

$B_o(\text{He}) = 4.88 \times 10^{-7}$ cm^2
$B_o(\text{Ar}) = 5.05 \times 10^{-7}$ cm^2
$B_o(CO_2) = 4.40 \times 10^{-7}$ cm^2

The average value to B_o was calculated to be:

$\bar{B}_o = (4.78 \pm 0.25) \times 10^{-7}$ cm^2

The linearly in Fig. 1 implies the constancy of B and/or χ. To test this the ratio F_o/ϕ was calculated for all the points. It was found that χ was not constant but varied in a regular manner *i.e.* it decreased with increasing ϕ and/or F_o. Although no

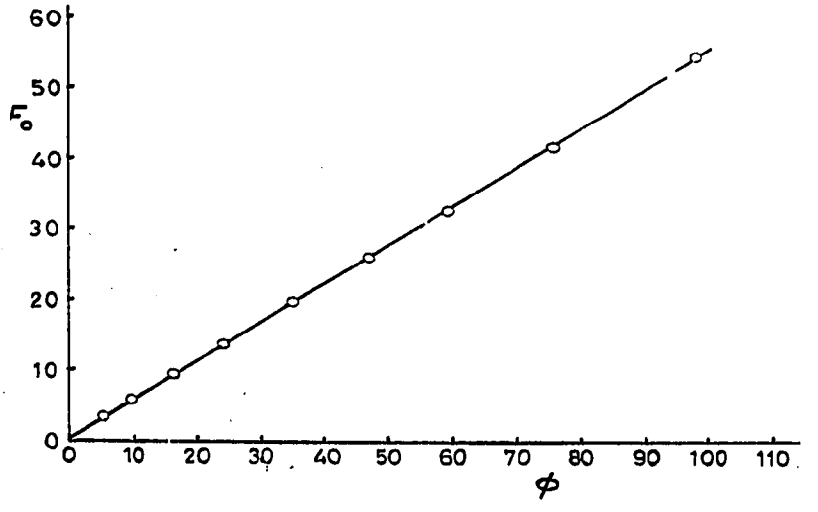

Fig. 1. F_o as a function of ϕ for He I.

present theory warrants it, it was found that χ could be plotted against $\bar{P}$ (the mean column pressure as defined by MARTIRE AND LOCKE[18]) to give a straight line fit. It was somewhat surprising to find this relationship to hold also for Ar and CO_2. Such plots

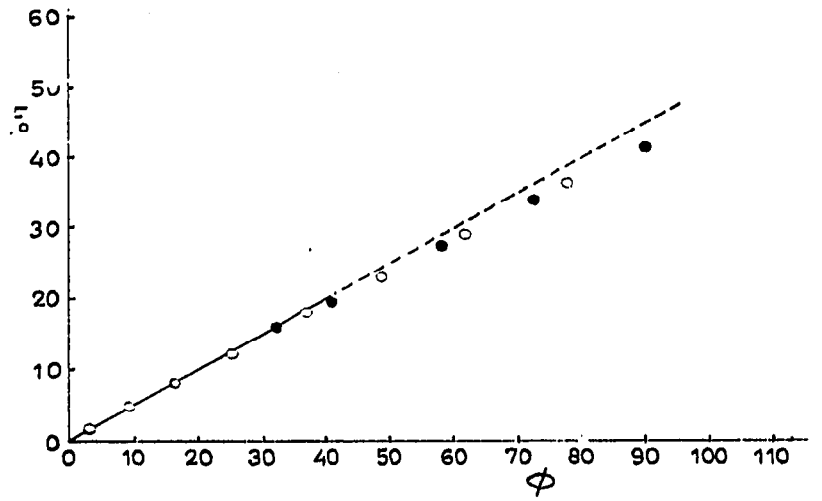

Fig. 2. F_o as a function of ϕ for Ar(II and III). ○ = Ar II; ● = Ar III.

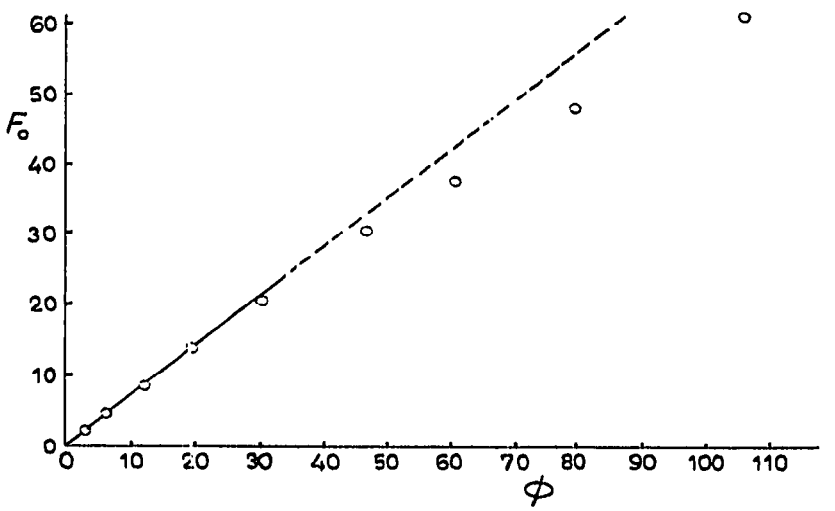

Fig. 3. F_o as a function of ϕ for CO_2 I.

are shown in Figs. 4–6 for He (I and II), Ar (II and III) and CO_2 I, respectively. In all three cases the relationship between χ and P was found to be

$$\chi = \chi_o - m\bar{P} \tag{28}$$

or more specifically from the least squares analysis the following three expressions were obtained:

$$\chi(\mathrm{He}) = 0.602 - 0.00666\ \bar{P} \tag{29}$$

$$\chi(\mathrm{Ar}) = 0.531 - 0.00794\ \bar{P} \tag{30}$$

$$\chi(\mathrm{CO_2}) = 0.809 - 0.0247\ \bar{P} \tag{31}$$

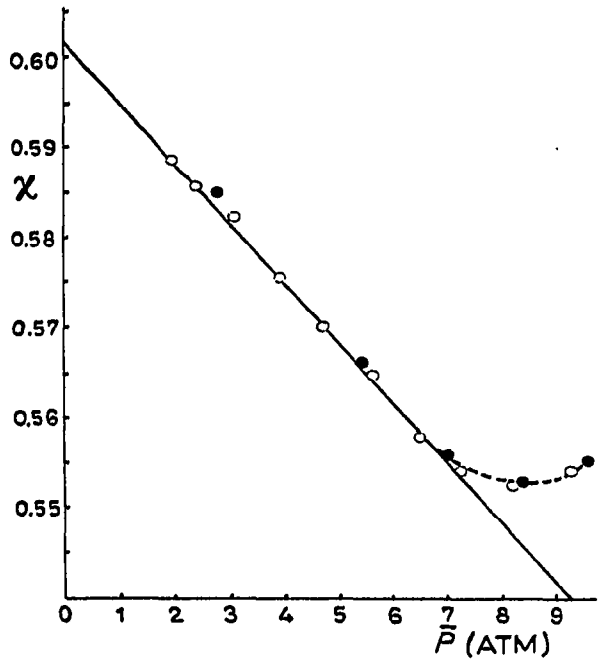

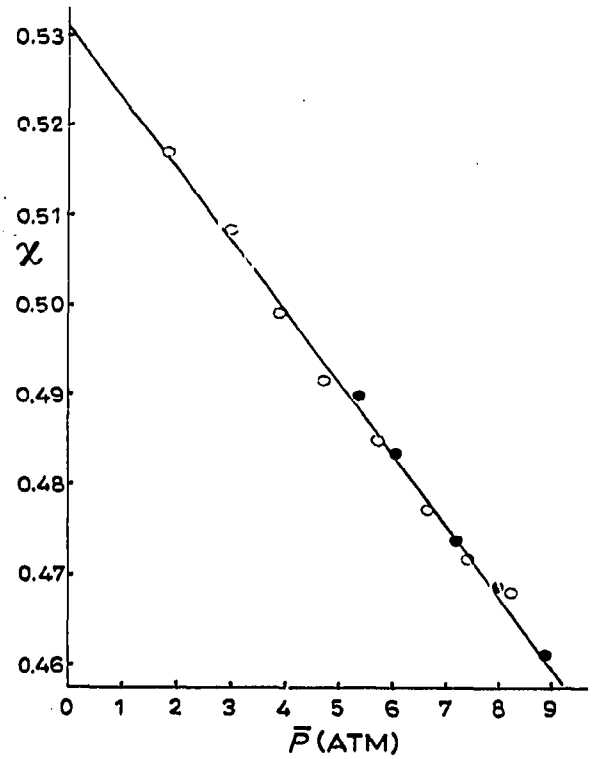

Fig. 4. χ as a function of $\bar{P}$ for helium carrier gas. ○ = He I; ● = He II.

Fig. 5. χ as a function of $\bar{P}$ for Ar(II and III). ○ = Ar II; ● = Ar III.

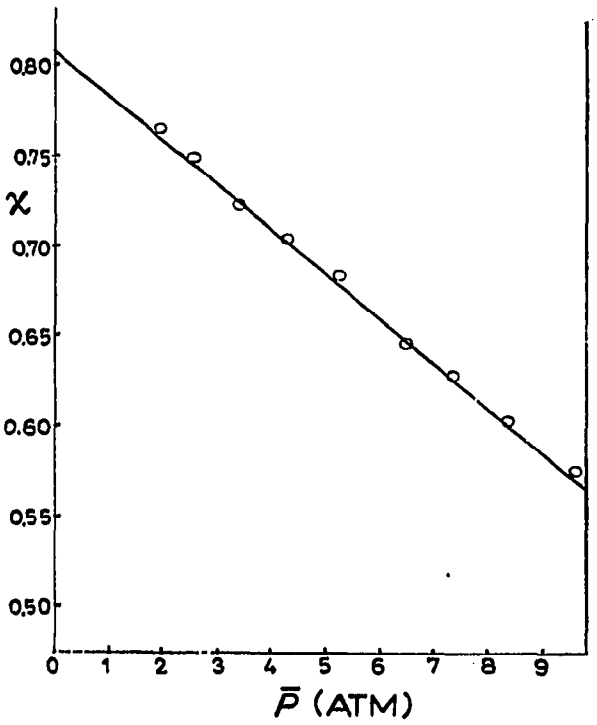

Fig. 6. χ as a function of $\bar{P}$ for CO_2 I.

From the χ_o values (χ at $\bar{P} = 0$ or very low flow rates where Darcy's Law is definitely valid) the following B_o values were obtained.

$$B_o(\text{He}) = 5.32 \times 10^{-7} \text{ cm}^2$$
$$B_o(\text{Ar}) = 5.24 \times 10^{-7} \text{ cm}^2$$
$$B_o(CO_2) = 5.23 \times 10^{-7} \text{ cm}^2$$

The average B_o was found to be

$$\overline{B_o} = (5.26 \pm 0.04) \times 10^{-7} \text{ cm}^2$$

The value is somewhat higher than that obtained from the slopes and has a spread of only 0.76 % compared to 5.23 %.

Perhaps the most unusual feature of Figs. 4–6 is the minima found in Fig. 4. Repeated experiments consistently showed the presence of this minima (this is shown in Fig. 4 by only one of the several repeated experiments, He II). The presence of this minima suggests that either the mechanism responsible for decreasing χ(or B) with mean column pressure begins to break down at elevated helium $\bar{P}$ or that a secondary mechanism working in the opposite direction becomes effective at $\bar{P}$ of about 7 atm. This deviation from the "normal" trend is coincidental with that observed in the V_N* (net retention volume corrected for carrier gas nonideality) *vs.* $\bar{P}$, and θ (apparent fraction of surface covered by the carrier gas) *vs.* $\bar{P}$ plots contained in the previous article[1]. Since χ is not directly related to V_N* (and in turn θ), then the first suggested reason for the presence of the minima must be dismissed. More clearly, in its simplest form V_N* is a function of F_o, t_R, and j and at constant pressure drop across the column the effect of changing χ will be only to alter F_o and t_R, but these vary in such a way so as to keep V_N* constant.

The secondary mechanism which is probably responsible for the coincidental departure must be such as to affect both χ and V_N* (or θ) simultaneously. It must be remembered that the anomalous effect is observed only in the helium case, indicating that only helium can participate in this type of mechanism. If it can be assumed that helium being of the right size and/or having the property such that at elevated pressure drops certain channels become permeable to it then the flow through the column will be somewhat greater than that predicted by eqns. 28 and 12 combined. Since F_o is the total flow measured at the column outlet, then from the definition of χ there will be an increase in χ (above that predicted by eqn. 29) proportional to the magnitude of the secondary flow.

If we define F_n and F_s as the normal interparticle flow and the secondary flow respectively, and if for the present we assume gas ideality, then essentially the net retention volume was calculated in ref. 1 by:

$$V_N = t_R j(F_n + F_s) - V_M \tag{32}$$

where as in ref. 1 V_M is the column volume accessible to the carrier gas and $(F_n + F_s)$ is merely F_o. Now, since methane like Ar and CO_2 cannot participate in the secondary flow then it is incorrect to use F_o in the calculation of V_N. The correct expression for V_N should be

$$V_N = F_n t_R j - V_M \tag{33}$$

and consequently V_N as calculated by eqn. 32 is larger than the true value by $F_s t_R j$.

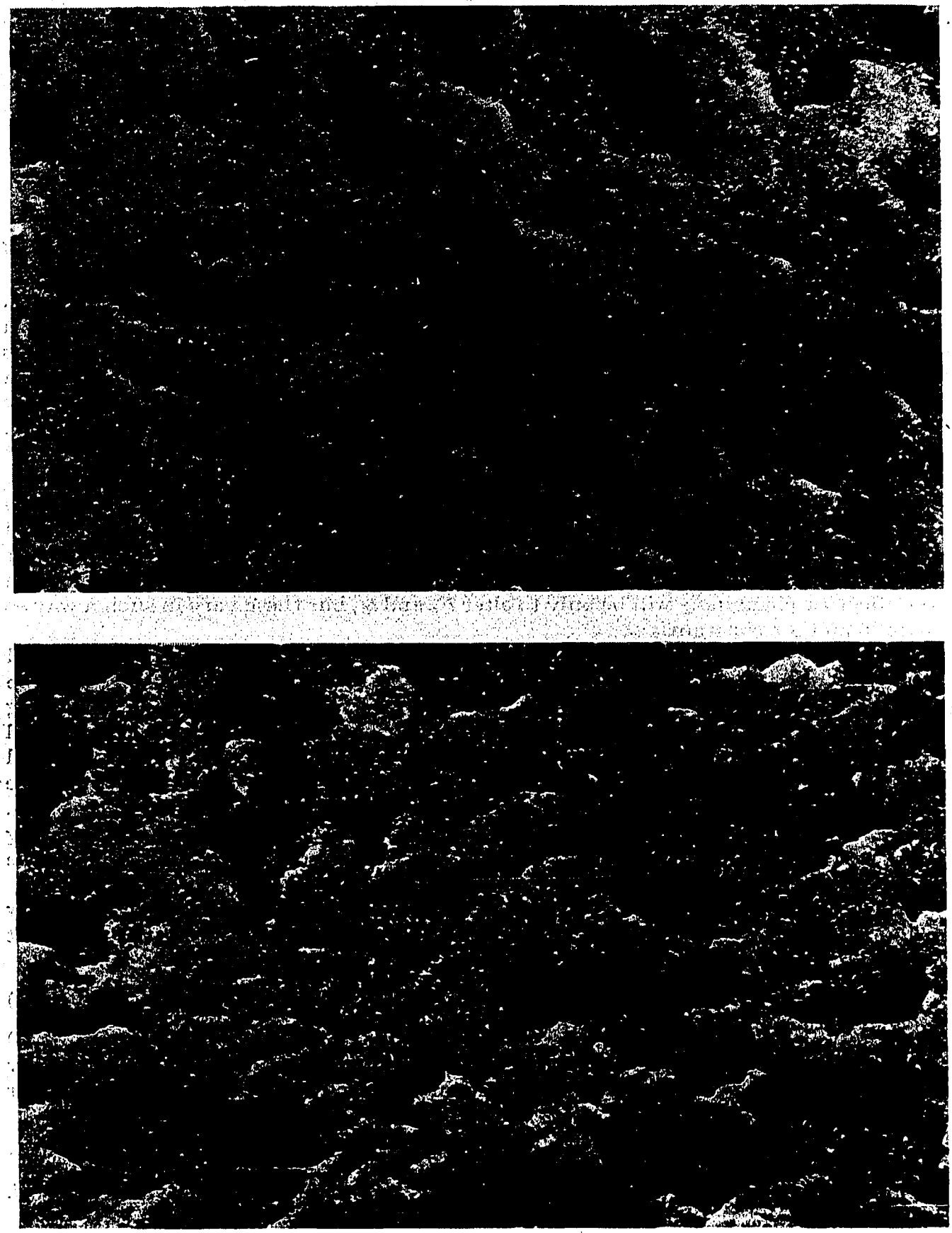

Fig. 7. Electronmicrographs of Porapak S.

Since F_s is expected to increase with increasing pressure drop, so will this difference. This is what is observed experimentally.

The secondary flow mechanism seems to satisfy, at least qualitatively, the experimental data. The limited range of this anomalous effect and the experimental scatter make a quantitive discussion fruitless. More can and will be said when the experimental range is extended to much higher $\bar{P}$.

The interparticle porosity was calculated from eqn. 14 (constant factor of 1/180) and eqn. 15 (constant factor at 1/150) using $B_o = 5.26 \times 10^{-7}$ cm^2 and $d_p = 0.02$ cm and was found to be 0.427 and 0.410, respectively. The total porosity was calculated from eqn. 16. V_M and V_T ($\pi r^2 L$) were found to be 89.5 and 130.5 cc, respectively, thus making $\varepsilon_T = 0.685$. Comparing this to the average of the interparticle porosity ($\varepsilon = 0.419$) shows that although the particles appear to be smooth and spherical under low magnification ($\sim 30 \times$) they are indeed quite porous ($\Delta \simeq 0.267$). In fact the particle porosity is calculated to be about 0.47 which means that at least 47 % of the particle is empty space. This is in good agreement with the electronmicrographs shown in Fig. 7.

In order to test whether the present experimental data is governed by the Ergun relationship, $1/B$ was plotted against F_o. These plots are shown in Figs. 8–10 for He I, Ar II and CO_2 I, respectively. Included in each figure is the plot of eqn. 23 as well as the Reynolds number.

As can be seen in all three figures there is very little (if any) resemblance between the experimental curves and those dictated by the Ergun equation. All three figures show that the permeability coefficient decreases at a much faster rate than that predicted by eqn. 23, this being particularly true for the low flow rate region. In the case of Ar and CO_2, however, the slopes of the experimental curves do decrease and begin to approach those of the Ergun equation as the flow is increased. This may also be true in the helium case but the undue increase in permeability masks this.

One feature common to all three figures is the break in the curve at F_o of about

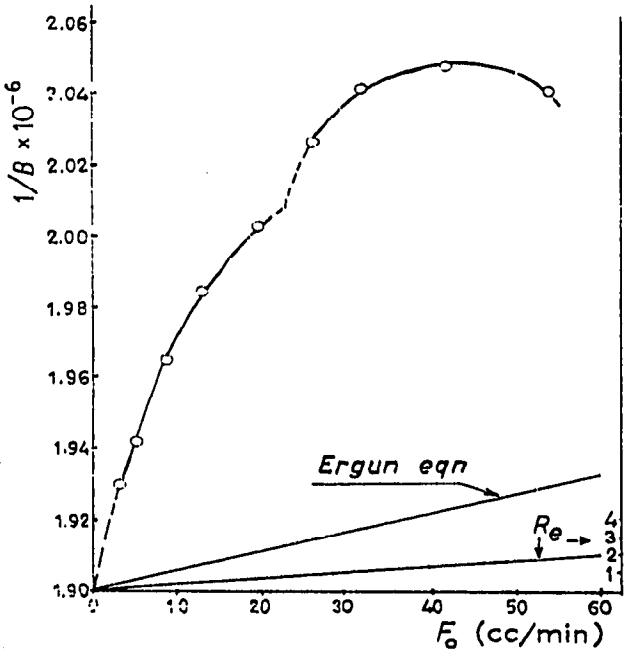

Fig. 8. $1/B$ as a function of F_o for He I.

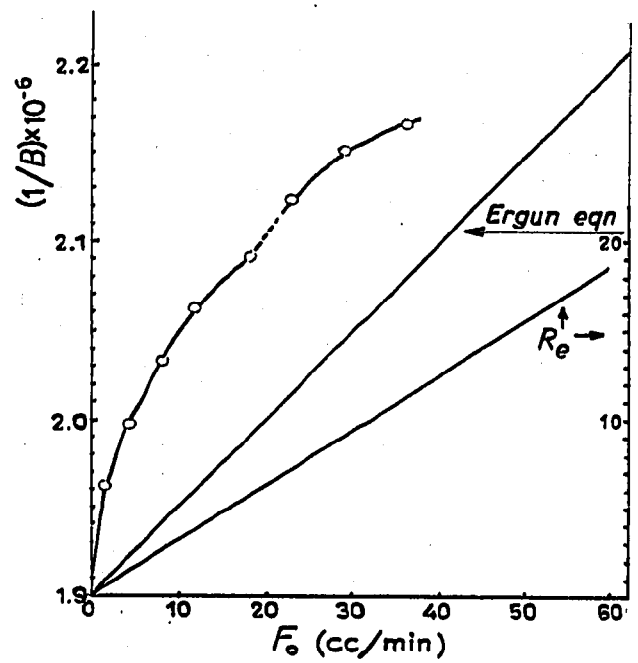

Fig. 9. $1/B$ as a function of F_0 for Ar II.

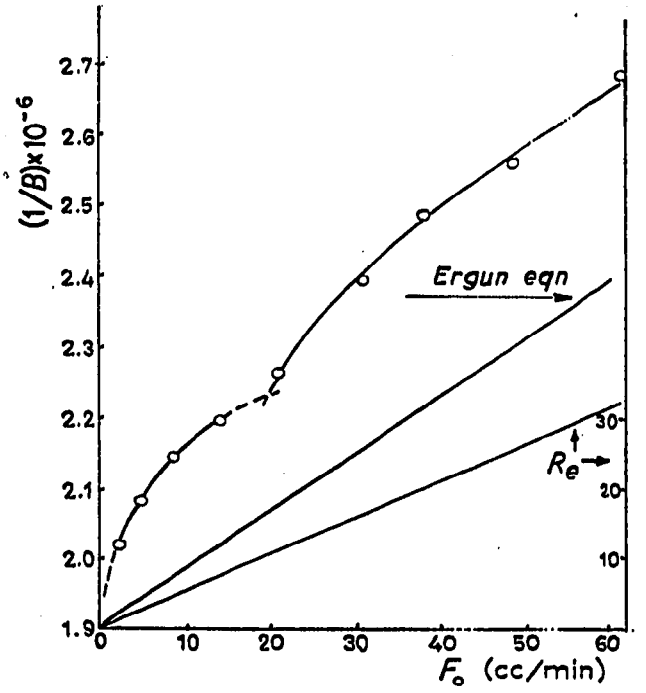

Fig. 10. $1/B$ as a function of F_0 for CO_2 I.

20 cc/min. This cascading variation may be the result of flow induced decrease of interparticle porosity in the individual sections of the column (it must be remembered that the resulting 200 ft. column is made up of four terminated 50 ft. sections). This is not unreasonable if one considers that in the vicinity of $\varepsilon = 0.4$ a 1 % change in the interparticle porosity alters the permeability by some 5 %. From the three figures it would appear (if the mechanism is valid) that only two of the four sections are affected and these would necessarily be those closest to the column outlet where the gas velocity is the greatest.

All the experiments that have been carried out are grouped as follows. The first group contains He I, Ar II, Ar III and CO_2 I (these experiments have already been discussed) and the second group contains experiments Ar I, CO_2 II, CO_2 III and CO_2 IV. The basic difference between the two groups is the way in which the working inlet pressures were approached. In the first group an experiment was carried out by starting at the highest operating inlet pressure. After the completion of a run the pressure regulating valve was turned down by a suitable amount and the pressure was allowed to fall relatively slowly to the next highest operating pressure. All subsequent operating pressures were approached in the same way.

Experiment Ar I and CO_2 IV were carried out starting at the lowest inlet pressure and incrementally increasing it to highest value. Under these conditions the alteration of the pressure regulating valve resulted in a sudden inrush of gas into the column and as a result the column experienced a pressure pulse before it reached a steady state.

In experiment CO_2 II, the inlet pressure was first allowed to fall to about 4 p.s.i. above the atmospheric (4 p.s.i. + P_0), after which it was raised to the first operating

pressure (19.25 p.s.i. + P_o). After sufficient equilibrium time (~ 16 h) the first experiment was performed. The subsequent experiments were carried out as in Ar I and CO_2 IV.

The only difference between experiments CO_2 II and CO_2 III is that in experiment CO_2 III the inlet pressure was first allowed to fall to approximately (16 p.s.i. + P_o) after which it was raised to the first operating pressure (20.2 p.s.i. + P_o).

The results of the second group of experiments are summarised by plotting χ *vs.* $\bar{P}$ in Fig. 11 (Ar) and Fig. 12 (CO_2). For comparison Fig. 5 and Fig. 6 are also reproduced in Fig. 11 and Fig. 12, respectively. Comparing the results of the first group to those of the second group shows that the relationship between χ and $\bar{P}$ is not only dependent on whether the inlet pressure is altered in an increasing or decreasing direction but it also depends on the initial starting conditions (comparison of CO_2 II, CO_2 III and CO_2 IV).

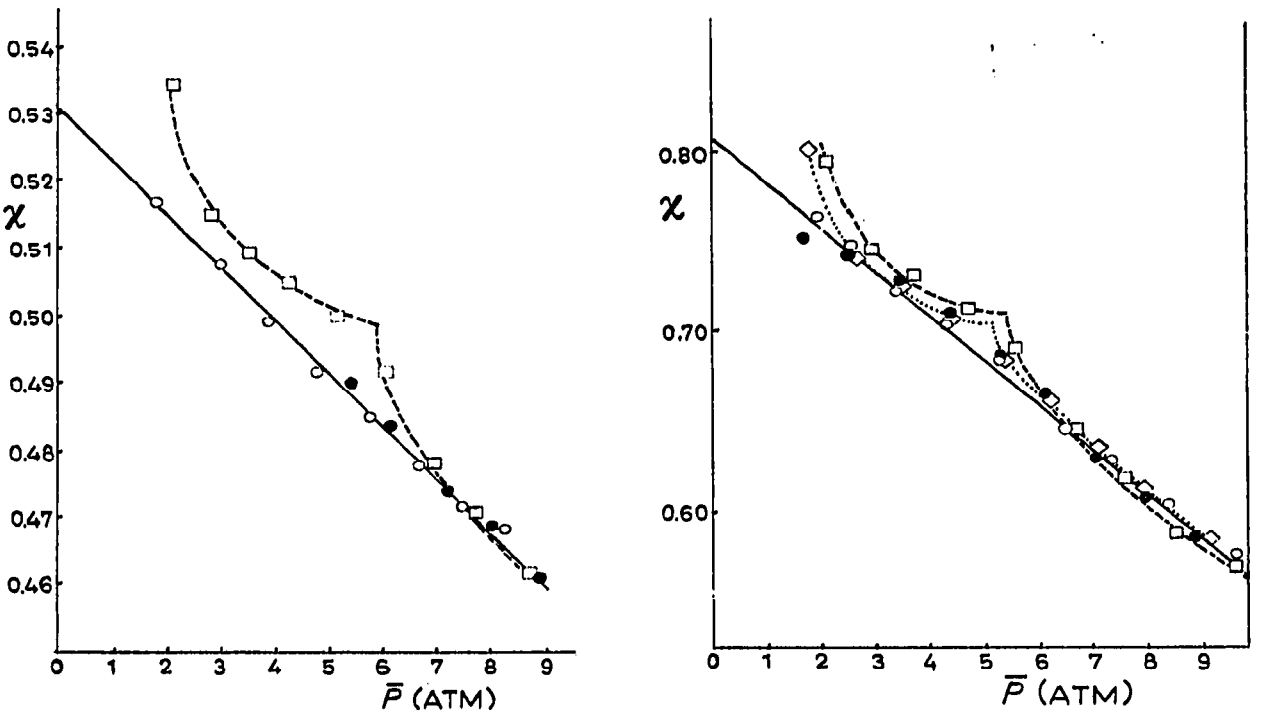

Fig. 11. χ as a function of $\bar{P}$ for Ar I and Ar(II and III). □ = Ar I; ○ = Ar II; ● = Ar III.

Fig. 12. χ as a function of $\bar{P}$ for CO_2 I, CO_2 II, CO_2 III and CO_2 IV. ○ = CO_2 I; ● = CO_2 II; ◇ = CO_2 III; □ = CO_2 IV.

The experiments Ar I, Ar II, CO_2 II, CO_2 III, CO_2 IV and Ar III were performed in the order written. Considering this and the fact that the experiments are reproducible leads to the conclusion that the column behaves as if though it possessed a permeability hysteresis. The term hysteresis serves here only to describe the fact that a different set of results are obtained by changing the direction in which the inlet pressure is altered. This hysteresis effect is not only found in the permeability study but it also appears in the plate height study. This is illustrated in Fig. 13 where $\hat{H}/f_2$ is plotted against $u_o P_o$ for the Ar I, Ar II, and Ar IV experiments where CH_4 was the

solute. A similar effect is also found for the CO_2 case but the inclusion of such a plot would be of no additional interest.

In both Figs. 11 and 12 the break in the curve is unmistakable. In both cases this break occurs at a $\bar{P}$ value close to 6 atm which corresponds to F_o of about 20 cc/min. In the first group of experiments the break in the curve was found in the $1/B$ *vs.* F_o plot whereas in the second group of experiments this is found in the χ *vs.* $\bar{P}$ plot.

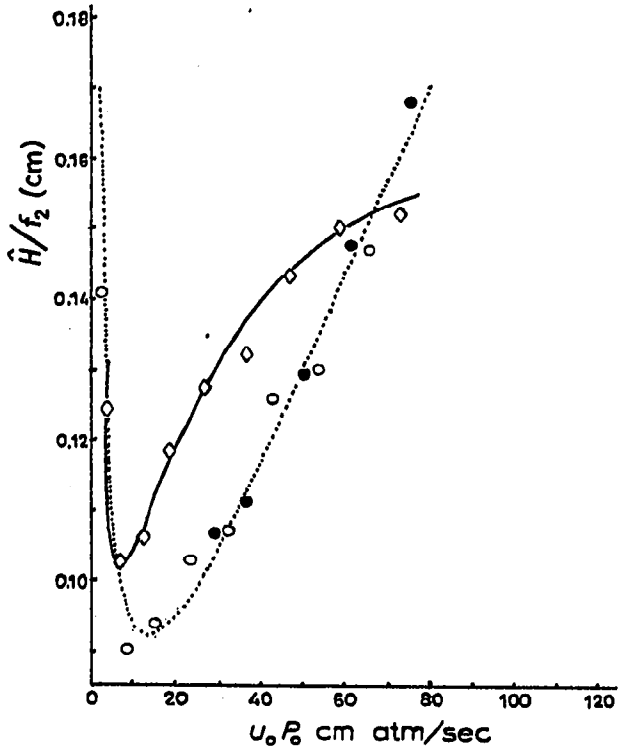

Fig. 13. Plot of $\hat{H}/f_2$ as a function of u_oP_o for Ar I and Ar(II and III). ◇ = Ar I; ○ = Ar II; ● = Ar III.

Finally a common $1/B$ *vs.* F_o plot for Ar and for CO_2 (not included) reveals that for either carrier gas although the individual experimental plots are non linear they do tend to approach a common straight line whose slope is somewhat similar to that predicted by the Ergun equation. The experimental scatter about this central line is not from experimental uncertainty for each point consists of about six flow rate measurements each with the reproducibility of better than $\pm$ 0.01 %. The experimental line is vertically displaced from the Ergun equation in the direction of higher $1/B$ suggesting that extrapolation from the high F_o region leads to a lower column permeability. This is in accord with the particle shift (compacting) proposal.

ACKNOWLEDGEMENTS

We wish to thank the National Research Council of Canada for the financial assistance. We would also like to thank Dr. P. K. ISAAC for the electron photomicrographs of Porapak S cross sections.

REFERENCES

1 J. J. CZUBRYT, H. D. GESSER AND E. BOCK, *J. Chromatog.*, 53 (1970) 439
2 L. PRANDTL, *Essentials of Fluid Dynamics*, Blackie, Glasgow, 1954, p. 102
3 Fluid Motion Memoirs: *Laminar Boundry Layers*, Rosenhead, Oxford (Clarendon Press), 1963, p. 121.
4 J. C. GIDDINGS, *Dynamics of Chromatography*, Part I, Marcel Dekker, New York, 1965, pp. 199–224.
5 P. C. CARMAN, *Flow of Gases Through Porous Media*, Butterworths, London, 1956.
6 H. PURNELL, *Gas Chromatography*, Wiley, New York, 1962, pp. 60–66.
7 G. GUIOCHON, *Chromatog. Rev.*, 8 (1966) 1
8 J. BOHEMAN AND J. H. PURNELL, *J. Chem. Soc.*, (1961) 360.
9 S. DAL NOGARE AND R. S. JUVET, Jr., *Gas–Liquid Chromatography*, Interscience, New York, 1962, p. 134.
10 R. B. BIRD, W. E. STEWART AND E. N. LIGHTFOOT, *Transport Phenomena*, Wiley, New York, 1960, p. 199.
11 D. A. WHITE, *Chem. Eng. Sci.*, 22 (1967) 669.
12 T. SEELY, *J. Polymer Sci.*, 5 (1967) 3029.
13 W. L. MCCABE AND J. C. SMITH, *Unit Operations of Chemical Engineering*, McGraw-Hill, New York, 1967, p. 161.
14 J. C. REISCH, C. H. ROBINSON AND T. D. WHEELOCK, in N. BRENNER, J. E. CALLEN AND M. D. WEISS (Editors), *Gas Chromatography*, Academic Press, New York, 1962, p. 91.
15 J. HALASZ AND H. D. GERLACH, *Anal. Chem.*, 38 (1966) 281.
16 G. L. HARGROVE AND D. T. SAWYER, *Anal. Chem.*, 39 (1967) 9115.
17 E. A. MOELWYN-HUGHES, *Physical Chemistry*, Pergamon Press, London, 1961, p. 610.
18 D. E. MARTIRE AND D. C. LOCKE, *Anal. Chem.*, 37 (1965) 144.